Limit – Solutions for the Heat Transfer in OPGW Submitted to Short-circuit Test

Sergio Colle[1], Marcelo A. Andrade[2], Mauro Bedia[2], João T. Pinho[3], Karime L. Z. Glitz[1], Carlos E. Veiga[1], and Júlio N. Scussel[1]

[1]Department of Mechanical Engineering / Federal University of Santa Catarina
Florianópolis, Santa Catarina, Brazil
+55-48-2342161 / 2340408 · colle@emc.ufsc.br
[2]Pirelli Telecomunicações Cabos e Sistemas do Brasil S.A.
Sorocaba – São Paulo – Brazil
+55-15-32359209 · marcelo.andrade@pirelli.com.br
[3]Department of Electric Engineering / Federal University of Pará
Belém – Pará – Brazil
+55-91-32111299 · jtpinho@ufpa.br

Abstract

The present paper focuses the unsteady heat transfer problem related to the thermal effects in an OPGW submitted to short-circuit current tests. Temperature gradients in the armored wires, in the aluminum tube, are predicted and compared with experimental results collected from two standardized short-circuit current test runs. The limit-solution corresponding to vanishing contact angles of the contact surface between the tube and the armored wires is derived and shown to be physically meaningful. The theoretical results presented here, is compared with the predicated results obtained from an analytical solution reported in the proceedings of the last IWCS conference. The conditions under which, the thermal capacitance model reported in a previous published work is in agreement with the predicted results of the present model is also discussed. Short-circuit test runs were carried out for an aluminum tube - galvanized steel wires OPGW. The thermal contact resistance parameter of the contact surface between the tube and the armored wires is estimated against the experimental data.

Keywords: OPGW, Short-circuit test; unsteady heat-transfer.

1. Introduction

The short-circuit current carrying capacity of an OPGW conductor of the type focused here, according to the cross section shown in Figure 1, depends mainly on the maximum temperature achieved in the aluminum tube. The temperature distributions over the cross section of the tube and the wires depend on the energy factor $I^2\Delta t$ as well as on the electric resistance of the tube and the armored wires. Previous work of the authors [1] presented an analytical solution for the temperature distribution in a closed form, which is supposed to be valid only for the special case of small thermal contact angle in the contact interface between the tube and the armored wires. The solution reported in [1] has shown to be in disagreement with the experimental results collected from a short-circuit test run of conductor Pirelli – OPGW – SM 13,4 6 FO. The maximum temperature achieved in the tube has proved in [1] to be dependent not only on the electric resistance of the tube and the wires but also on the thermal contact resistance between the tube and the wires. Furthermore it is also shown that the rate of cooling of the tube is sensitive with the thermal contact resistance. The thermal contact resistance geometric parameter is difficult to characterize because the mechanical contact between the armored wires and the tube is not uniform. The geometry of the contact surface basically depends on the conductor design as well as on the manufacturing process. Experimental results also show that the thermal contact resistance changes due to the thermal deformation of the armored wires, during the cooling phase of the short-circuit test. In order to take into account the prediction of the variation of the thermal contact resistance with time, a more general solution in proposed here. The present solution can be extended to the case of non-homogeneous OPGW conductors made of wires with different materials. The numerical scheme proposed here in order to solve the related non-linear equations is effective, and allows one to consider arbitrary polynomials of temperature-dependent electric resistance of the tube and the wires. In order to simplify the present analysis, it is further assumed here that the electric resistance of the wire is evaluated as a function of the average wire temperature over its cross section. The predicted results show that for the particular case of aluminum-galvanized-steel wires, the thermal gradient over the cross section of the wires cannot be neglected.

2. Basic Equations

In the present analysis the skin effects due to the intensive short-circuit current are neglected. The skin effect for an OPGW as focused here, according to [2], may result in a temperature difference over the cross section of the aluminum tube around 10°C. This temperature gradient is around 4% of the maximum temperature expected in the aluminum tube. It is assumed here that the heat loss at the outer surfaces of the armored wires to the surrounding medium is neglected. The optic fibers gel tube inside the aluminum tube is supposed to be thermally insulated. The temperature gradient over the cross section of the tube is also neglected.

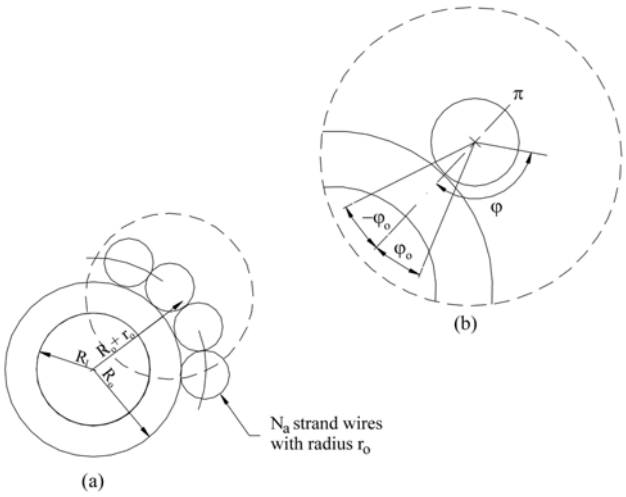

Figure 1. (a) Cross section geometry of OPGW
(b) Expanded view of the wire showing the contact angle

In a previous paper of the authors [1], the heat transfer problem of the OPGW conductor is posed and solved analytically, by assuming a small contact angle at the interface of thermal contact between the tube and the wires.

According to [1] the heat transfer in the OPGW is governed by the differential equations expressed in terms of dimensionless variables as given bellow.

2.1 Aluminum Tube

$$\alpha \frac{d\theta_i}{d\tau} = p_i(\theta_i, \bar{\theta}_a) - \frac{2}{\pi} F_{oa} N_a \sqrt{1+\lambda_a{}^2}\, \phi_o(\tau) \qquad (1)$$

where $\theta = \dfrac{T - T_o}{T_o}$, $\bar{\theta}_a$ is the average wire temperature over the wire cross section, $\eta = r/r_a$, $\phi(\varphi,\tau) = \dfrac{\partial \theta_a}{\partial \eta}(1,\varphi,\tau)$ is the dimensionless heat flux, $\phi_o = \int_0^{\varphi_o} \phi(\varphi,\tau) d\varphi$, $\tau = t/\Delta t_c$, T_o is the initial temperature, Δt_c is the short-circuit duration time, $\alpha = \rho_i c_i \pi \left(R_o{}^2 - R_1{}^2\right) \big/ \rho_a c_a \pi r_a{}^2$, ρ is the specific mass, c is the specific heat, $F_{oa} = k_a \Delta t_c \big/ \rho_a c_a r_a{}^2$ is the Fourier number of the wire, $p_i = (I^2 \Delta t_c) R_{20i} \lambda_r{}^2 f_i f_a{}^2 \big/ \left(f_i + \lambda_r f_a\right)^2 \rho_a c_a \pi r_a{}^2 L T_o$, $\lambda_r = \dfrac{R_{20a}}{N_a R_{20i}} = \left(\dfrac{\rho_{20a}}{\rho_{20i}}\right)(R_o{}^2 - R_1{}^2) \dfrac{\sqrt{1+\lambda_a{}^2}}{N_a r_a^2}$, $\lambda_a = \dfrac{2\pi R_o}{L}$, f_i and f_a are the electrical resistance temperature-depended functions of the aluminum and steel, respectively, R_{20} is the electrical resistance at 20°C and ρ_{20} is the electrical resistivity at 20°C.

Here $L_a = L\sqrt{1+\lambda_a{}^2}$ is the length of the effective thermal contact surface strip of width $e_a = 2 r_a \varphi_o$, N_a is the number of wires of the strand, k_a is the thermal conductivity of the wire material, r_a is the wire radius, R_o and R_1 are the inner and outer radii of the aluminum tube, respectively.

2.2 Armored Wires

$$\frac{1}{\eta}\frac{\partial}{\partial \eta}\left(\eta \frac{\partial \theta_a}{\partial \eta}\right) + \frac{p_a}{F_{oa}} = \frac{1}{F_{oa}} \frac{\partial \theta_a}{\partial \tau} \qquad (2)$$

where $p_a = (I^2 \Delta t) R_{20a} f_a f_i{}^2 \big/ \left(f_i + \lambda_r f_a\right)^2 \rho_a c_a \pi r_a{}^2 L_a T_o N_a{}^2$ and $F_{oa} = k_a \Delta t_c \big/ \rho_a c_a r_a{}^2$.

The boundary and interface conditions for equations (1) and (2) are given by

$$\frac{\partial \theta_a}{\partial \eta}(1,\varphi,\tau) = \phi(\varphi,\tau) \quad \text{for } -\varphi_0 \le \varphi \le \varphi_0 \;;\; \tau > 0 \qquad (3)$$

and

$$\frac{\partial \theta_a}{\partial \eta}(1,\varphi,\tau) = 0 \quad \text{for } |\varphi| > \varphi_0 \qquad (4)$$

The initial conditions are given by,

$$\theta_i(0) = \theta_a(\eta,\varphi,0) = 0 \qquad (5)$$

The thermal contact resistance in the interface between the wires and the tube is accounted for in the Biot number in the following equation [1],

$$\phi(\tau,\varphi) = -B_i\left(\theta_a(1,\varphi,\tau) - \theta_i(\tau)\right) \qquad (6)$$

where $B_i = h r_a / k_a$, where h is the heat transfer coefficient by conduction and convection in the effective heat transfer area.

The solution of equation (2) for the boundary conditions given by equations (3), (4) and (5) are obtained by the method of Green's functions for the Neumann problem, as presented in the Appendix. The mathematical background is given in [3] and [4].

The temperature distribution in the outer surface of the wire, $\theta_a(1,\varphi,\tau)$, according to equation (A6) of the Appendix can be written as follows,

$$\theta_a(1,\varphi,\tau) = \int_0^\tau p_a\left(\theta_i, \bar{\theta}_a\right) d\tau' + \frac{2F_{oa}}{\pi} \int_0^\tau \left\{ \int_0^{\varphi_0} \left[g_o(\tau,\tau') + \sum_{n=1}^{\infty} g_n(\tau,\tau') \cos n\varphi \cos n\varphi' \right] \phi(\varphi',\tau') \, d\varphi' \right\} d\tau' \qquad (7)$$

where

$$g_o(\tau,\tau') = 1 + \sum_{m=1}^{\infty} e^{-\beta_m^{o^2} F_{oa}(\tau-\tau')} \qquad (8)$$

$$g_n(\tau,\tau') = 2 \sum_{m=1}^{\infty} \frac{e^{-\beta_m^{n^2} F_{oa}(\tau-\tau')}}{(1 - n^2/\beta_m^{n^2})} \qquad (9)$$

where β_m^n is the root of the Bessel function of first kind of integer order $J_n'(\beta_m^n) = 0$; $n = 0, 1, 2 \ldots$.

The series expansion of the Green's function suggests to expressing the heat flux in terms of a Fourier series as follows,

$$\phi(\varphi,\tau) = c_o(\tau) + \sum_{n=1}^{\infty} c_n(\tau) \cos n\varphi \qquad (10)$$

where $c_o(\tau) = \dfrac{1}{\pi}\phi_o$, $c_n(\tau) = \dfrac{2}{\pi}\phi_n$, where

$\phi_n(\tau) = \int_0^{\varphi_0} \phi(\varphi,\tau) \cos n\varphi \, d\varphi$, n = 0,1,2… so that $\phi(\varphi,\tau) = 0$ $\varphi > \varphi_o$.

From an energy balance in the wire it can be shown that the average temperature over the cross section of the wire can be expressed as

$$\frac{d\bar{\theta}_a}{d\tau} = p_a(\theta_i, \bar{\theta}_a) + \frac{2F_{oa}}{\pi}\phi_o(\tau) \tag{11}$$

From equation (5) it follows that the initial condition for equation (11) is $\bar{\theta}_a(0) = 0$.

By direct integration of equation (6) multiplied side by side by $\cos p\varphi$ in the interval $[0, \varphi_0]$, the following integral equation in terms of ϕ_n, n = 1, 2,.., N is obtained for the case of p = 0,

$$\begin{aligned} &\frac{\phi_o(\tau)}{\Lambda} + \int_0^\tau g_o(\tau,\tau')\phi_o(\tau')d\tau' \\ &+ \sum_{n=1}^{N} \frac{sen\, n\varphi_o}{n\varphi_o} \int_0^\tau g_n(\tau,\tau')\phi_n(\tau')d\tau' \\ &= \frac{\pi}{2F_{oa}}\left[\theta_i(\tau) - \int_0^\tau p_a(\theta_i, \bar{\theta}_a)d\tau'\right] \end{aligned} \tag{12}$$

while for p = 1, 2, .., N,

$$\begin{aligned} &\frac{\phi_p(\tau)}{\Lambda} + \int_0^\tau \left(\frac{sen\ p\varphi_o}{p\varphi_o} g_o(\tau,\tau')\phi_o(\tau') \right. \\ &\left. + \sum_{n=1}^{N} g_n(\tau,\tau')A_{np}\phi_n(\tau') \right) d\tau' \\ &= \frac{sen\ p\varphi_o}{p\varphi_o} \frac{\pi}{2F_{oa}}\left[\theta_i(\tau) - \int_0^\tau p_a(\theta_i(\tau')), \bar{\theta}_a(\tau')d\tau'\right] \end{aligned} \tag{13}$$

where $A_{np} = A_{pn} = \frac{1}{\varphi_o}\int_0^{\varphi_0} \cos n\varphi \cos p\varphi\, d\varphi$,

$$A_{np} = \frac{1}{2\varphi_o}\left(\varphi_o + \frac{sen\ 2n\varphi_o}{2n}\right) \quad ; n = p \tag{14}$$

$$A_{np} = \frac{1}{2\varphi_o}\left(\frac{sen(n-p)\varphi_o}{n-p} + \frac{sen(n+p)\varphi_o}{n+p}\right) \tag{15}$$
$$; n \neq p \quad ; n, p = 1,2,..., N$$

where $\Lambda = \frac{2F_{oa}\varphi_o B_i}{\pi\alpha} = \frac{2F_{oa}(r_a\varphi_o h/k_a)}{\pi\alpha} = \frac{B_{ic}}{\alpha}$, and $B_{ic} = \frac{e_a h \Delta t_c}{\rho_a c_a \pi r_a^2}$.

B_{ic} is a parameter that accounts for the thermal contact resistance in the contact interface between the wires and the tube, which is proportional to the unknown film coefficient *h*, and the unknown effective contact angle φ_o.

The unknown functions related to equations (1), (11), (12), and (13) are $\theta_i(\tau), \bar{\theta}_a(\tau)$, and $\phi_n(\tau)$; n = 1, 2,…, *N*. These equations are non-linear because p_i e p_a depend on the temperatures $\theta_i(\tau)$ and $\bar{\theta}_a(\tau)$.

3. Numerical Scheme

Equations (1) and (11) are solved numerically by the Runge – Kutta fourth order method [4]. The heat flux unknown functions $\phi_n(\tau)$; n = 1, 2, .. , N are approximated by polygonal functions. For each n, $\phi_n(\tau)$ is expressed by a tent-function as defined below.

For the sub-interval $[\tau_{j-1}, \tau_j]$

$$\phi = \phi_j(\tau) = \frac{a_j(\tau - \tau_{j-1})}{\Delta\tau}; \Delta\tau = \tau_j - \tau_{j-1} \tag{16}$$

wile for the sub-interval $[\tau_j, \tau_{j+1}]$

$$\phi = \phi_j^+(\tau) = \frac{a_j(\tau + \Delta\tau - \tau)}{\Delta\tau}; \Delta\tau = \tau_{j+1} - \tau_j \tag{17}$$

where a_j is unknown. A polygonal element construction is shown in Figure 2.

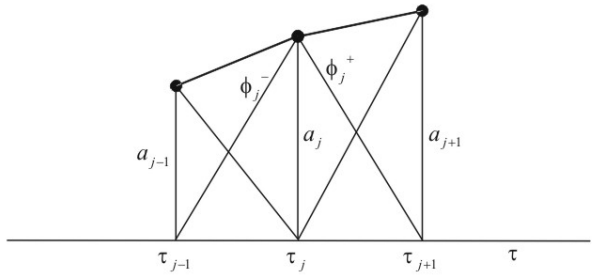

Figure 2. Composition of tent-functions for polygonal approximations of the heat flux

3.1 Case of Large Contact Angle

By performing the integrations in time of the integral terms of the left hand side of equations (12) and (13), the following equations are obtained respectively

$$\begin{aligned} &\left(\frac{1}{\Lambda} + \frac{\Delta\tau}{2} + B_{kk}^-\right)a_{ok} + 2\sum_{n=1}^{N}\left(\frac{sen\, n\varphi_o}{n\varphi_o}\right)B_{nkk}^-\, a_{nk} \\ &= \frac{\pi}{2F_{oa}}\left[\theta_i(\tau_k) - \int_0^{\tau_k} p_a(\theta_i, \bar{\theta}_a)d\tau'\right] \\ &- \sum_{j=1}^{k-1}\left[(\Delta\tau + B_{kj}^- + B_{kj}^+)a_{oj}\right. \\ &\left. + 2\sum_{n=1}^{N}\left(\frac{sen\, n\varphi_o}{n\varphi_o}\right)(B_{nkj}^- + B_{nkj}^+)a_{nj}\right] \end{aligned} \tag{18}$$

for p = 0 and

$$\frac{a_{pk}}{\Lambda}+\left(\frac{sen\ p\varphi_o}{p\varphi_o}\right)\left(\frac{\Delta\tau}{2}+B_{kk}^{-}\right)a_{ok}+2\sum_{n=1}^{N}B_{nkk}^{-}\ A_{np}\ a_{nk}$$
$$=\frac{\pi}{2F_{oa}}\left(\frac{sen\ p\varphi_o}{p\varphi_o}\right)\left[\theta_i(\tau_k)-\int_0^{\tau_k}p_a(\theta_i,\bar{\theta}_a)d\tau'\right]$$
$$-\sum_{j=1}^{k-1}\left[\frac{sen\ p\varphi_o}{p\varphi_o}(\Delta\tau+B_{kj}^{-}+B_{kj}^{+})a_{oj}\right.$$
$$\left.+2\sum_{n=1}^{N}A_{np}(B_{nkj}^{-}+B_{nkj}^{+})a_{nj}\right] \qquad (19)$$

for p = 1, 2, .., N .

The matrix coefficients appearing in equations (18) and (19) are given in the Appendix. The integrals in terms of p_a in the right hand side of these equations are performed numerically by the Sinpson´s rule.

Equations (18) and (19) can be cast in a matrix form as follows,

$$[H]\{a_{pk}\}=\{E_{pk}-S_{pk}-P_{pk}\} \qquad (20)$$

where

$$[H]=\begin{bmatrix}H_{oo} & H_{on}\\ H_{po} & H_{pn}\end{bmatrix}\quad ;\quad n,p=1,2,...N \qquad (21)$$

$$H_{oo}=\frac{1}{\Lambda_a}+\frac{\Delta\tau}{2}+B_{kk}^{-} \qquad (22)$$

$$H_{on}=2\frac{sen\ n\varphi_o}{n\varphi_o}B_{nkk}^{-} \qquad (23)$$

$$H_{po}=\frac{sen\ p\varphi_o}{p\varphi_o}\left(\frac{\Delta\tau}{2}+B_{kk}^{-}\right)\quad ;\quad p=1,2,...,N \qquad (24)$$

$$H_{pn}=\frac{\delta_{pn}}{\Lambda_o}+2A_{pn}B_{nkk}^{-}\quad ;\quad n,p=1,2,...,N \qquad (25)$$

$$E_{pk}=\frac{sen\ p\varphi_o}{p\varphi_o}\frac{\pi}{2F_{oa}}\theta_i(\tau_k)\quad ;\quad p=0,1,2,...,N \qquad (26)$$

$$S_{pk}=\frac{\pi}{2F_{oa}}\left(\frac{sen\ p\varphi_o}{p\varphi_o}\right)\int_0^{\tau_k}p_a(\theta_i,\bar{\theta}_a)d\tau' \qquad (27)$$

where $\frac{sen\ p\varphi_o}{p\varphi_o}=1$ for $p=0$

Equation (20) is used recursively to calculate the numerical coefficients a_{nj} , n = 0,1,2, .. , N ; j = 1, 2, .. , M , where M is the number of time steps.

The recursive matrix P_{pk} is given by

$$P_{pk}=\begin{cases}\sum_{j=1}^{k-1}(\Delta\tau+B_{kj}^{-}+B_{kj}^{+})\,a_{oj}\\ +2\sum_{n=1}^{N}\frac{sen\ n\varphi_o}{n\varphi_o}\sum_{j=1}^{k-1}(B_{nkj}^{-}+B_{nkj}^{+})a_{nj}\quad ;\quad p=0\\ \sum_{j=1}^{k-1}\left\{\frac{sen\ p\varphi_o}{p\varphi_o}(\Delta\tau+B_{kj}^{-}+B_{kj}^{+})\,a_{oj}\right.\\ \left.+2\sum_{n=1}^{N}A_{np}(B_{nkj}^{-}+B_{nkj}^{+})a_{nj}\right\}\quad ;\quad p=1,2,...N\end{cases} \qquad (28)$$

3.2 Limit-Solution for Vanishing Contact Angle

By taking the limit of equations (18) and (19) for φ_o tending to zero, and by assuming that the limit of Λ is some finite value Λ_o , it can be shown that $a_{nk}=a_{ok}$, n = 1,2, .., N , $A_{pq}=1$; p, q = 1,2, .., N , and that the matrix entries given by equations (22), (23), (24), and (25) assume respectively the forms

$$H_{oo}=\frac{1}{\Lambda_o}+B_o \qquad (29)$$

where $B_o=\frac{\Delta\tau}{2}+B_{kk}^{-}$,

$$H_{on}=2B_{nkk}^{-}=B_n\quad ;\quad n=1,2,...,N \qquad (30)$$

$$H_{po}=B_o\quad ;\quad p=1,2,...,N \qquad (31)$$

$$H_{pn}=\frac{\delta_{pn}}{\Lambda_o}+B_n\quad ;\quad n,p=1,2,...,N \qquad (32)$$

$$P_{ok}=\sum_{j=1}^{k-1}\left[\Delta\tau+B_{kj}^{-}+B_{kj}^{+}+2\sum_{n=1}^{N}(B_{nkj}^{-}+B_{nkj}^{+})\right]a_{oj} \qquad (33)$$

Furthermore $P_{pk}=P_{ok}$, $D_{pk}=D_{ok}$, and $S_{pk}=S_{ok}$; $p=1,2,...,N$.

In this case the recursive equation (20) reduces to

$$\left(\frac{1}{\Lambda_o}+\frac{\Delta\tau}{2}+B_{kk}^{-}+2\sum_{n=1}^{N}B_{nkk}^{-}\right)a_{ok}=E_{ok}-S_{ok}-P_{ok} \qquad (34)$$

; $k=1,2,...,M$.

4. Discussion of Results

Equations (1), (11), and (20) or (34) for case 3.2, are solved numerically. The corrector-predictor step given by the Runge-Kutta scheme, is applied to equations (1) and (11), after $\phi_o(\tau_k)=a_{ok}$ is solved in terms of θ_i and $\bar{\theta}_a$ from equation (20).

The predicted results for the conductor Pirelli – OPGW – SM 13,4 6 FO is shown in Figures 3, 4 and 5. The comparison of the predicted results with the experimental results obtained from two

independent short-circuit test runs is shown in Figures 6, 7, 8, and 9. Figure 3 illustrates the effect of the contact angle φ_o on the temperature rise during the heating time interval of the conductor. For any contact angle, it is supposed here that the material of the tube fills all the space limited from the inner radius and the armored wires. It is seen that large contact angles contribute substantially to reduce the temperature rise. It is shown that this effect becomes smaller the smaller the values of parameter B_{ic}.

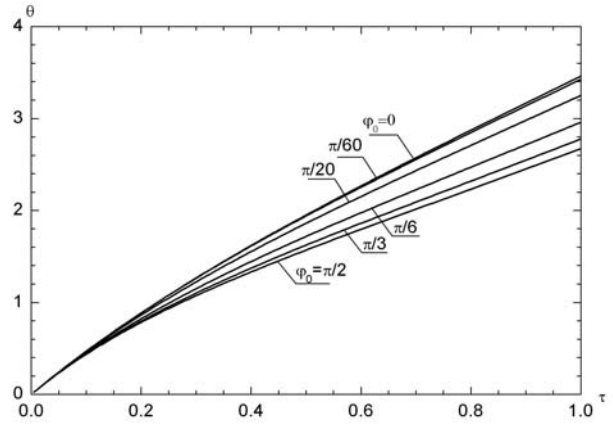

Figure 3. Predicted temperature distribution for the heating time interval, for various values of the contact angle φ_o, $B_{ic}=1$, and $N=20$

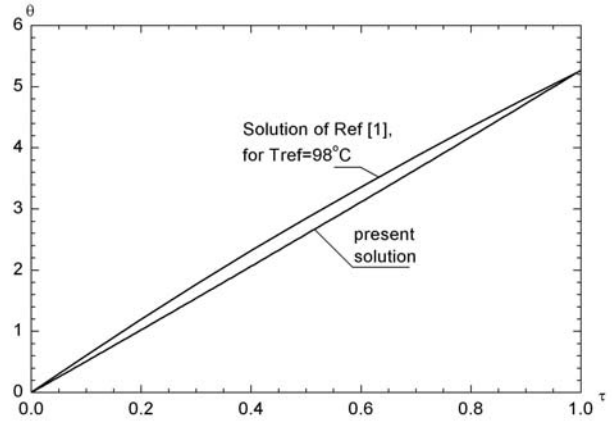

Figure 4. Predicted temperature distribution in the tube obtained by the present solution compared to the solution obtained from a simplified solution given in [1], for $\varphi_o=\pi/64$, by assuming the electric resistances evaluated at an equivalent temperature equal to 98°C

Figure 4 shows the comparison of the results obtained here with the results obtained by a simplified solution presented by the authors in [1], for which the electric resistances of the tube and the wires are assumed to be constant and evaluated at an equivalent temperature equal to 98°C. As seen in Figure 4, the non-linear solution slightly differs from the constant equivalent electric resistance solution.

The effect of the contact angle in the interface between the tube and the wire on the maximum temperature achieved in the tube is illustrated in Figure 5. This figure shows that good thermal contact and large angle values are effective in reducing the maximum temperature achieved in the tube. Both Figures 3 and 5 also show that the present solution smoothly converges to the limit-solution corresponding to vanishing contact angle (case 3.2).

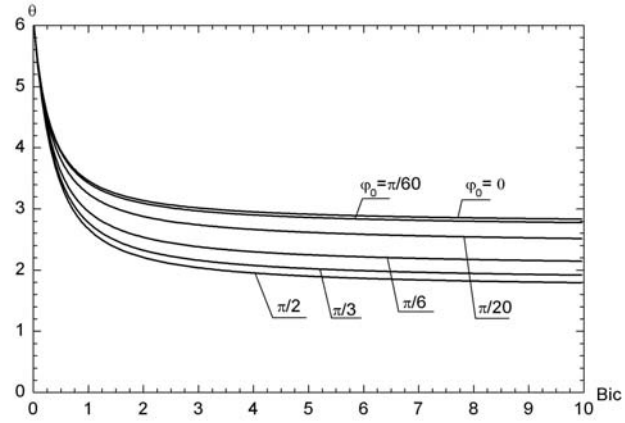

Figure 5. Predicted maximum temperature achieved in the tube for various values of the contact angle φ_o, as a function of the thermal contact resistance parameter B_{ic}

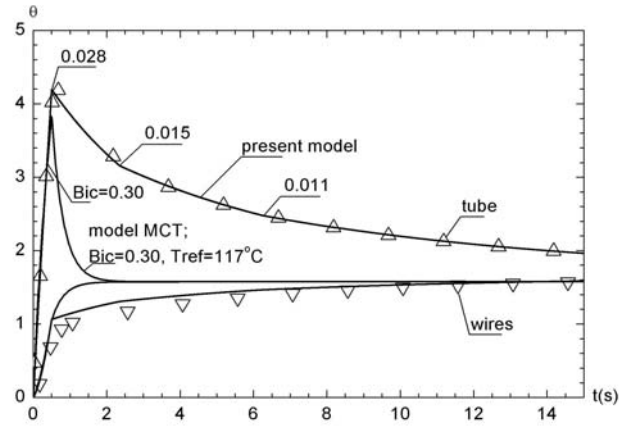

Figure 6. Predicted temperature distributions in the tube (upper) and the wire (lower) fitted piecewise with parameter B_{ic}, compared to the experimental results of the temperature in the outer surface of the tube, obtained in the first test, for $\Delta t_c = 0{,}5s$ and $I = 7{,}7kA$

The comparison of the predicted results with results obtained from a simplified solution, by assuming only thermal capacitance effects is illustrated in Figure 6. The results predicted by the thermal capacitance model (MCT) are also plotted in Figure 6. It is shown from this figure that the MCT model underestimates the maximum temperature achieved in the tube, by around 25°C. The MCT model also underestimates the temperature of the tube during the cooling time period. This disagreement could be reduced by splitting the

MCT solution in two branches, each of which corresponding to a particular numerical value of B_{ic}.

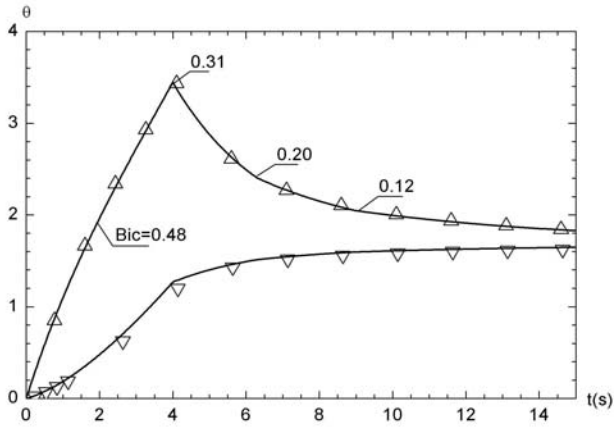

Figure 7. Predicted temperature distributions in the tube (upper) and the wire (lower) fitted piecewise with parameter B_{ic}, compared to the experimental results of the temperature in the outer surface of the tube, obtained in the first test, for $\Delta t_c = 4s$ and $I = 2{,}72kA$

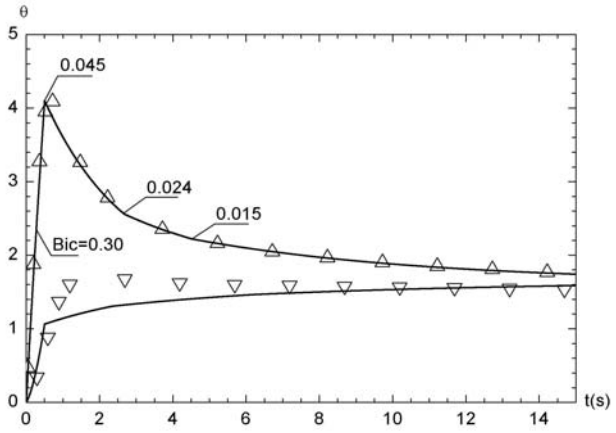

Figure 8. Predicted temperature distributions in the tube (upper) and the wire (lower) fitted piecewise with parameter B_{ic}, compared to the experimental results of the temperature in the outer surface of the tube, obtained in the second test, for $\Delta t_c = 0{,}5s$ and $I = 7{,}7kA$

The solution presented here is fitted against the experimental data by adjusting parameter B_{ic} piecewise. The fitted prediction curves are compared with the experimental results in Figure 6, 7, 8, and 9. These figures show the predicted results are in good agreement with the experimental results in terms of the tube temperature. Figures 6, and 7 show also good agreement with respect to the wire temperature.

Figures 8 and 9 show the comparison of the predicted results with the experimental results corresponding to the second test run. It is seen from these figures that the fitted values of the thermal contact resistance parameter B_{ic} are closed to each other.

Figure 8 shows that the predicted results for the wire temperature are not in good agreement with the experimental results. It should be mentioned here that in the second test run, the armored wires were kept tightly fixed against the aluminum tube by means of a stiff thermo-plastic ring, in the conductor section where the thermocouples were installed. The overestimation of the predicted wire temperature may be explained by the fact that the tube heats up less intensively while the wires heat up more intensively in the case of the second test run, than in the first one. These results may also explain why the B_{ic} number corresponding to the second test run, as seen in Figure 9, is slightly bigger than the B_{ic} number corresponding to the first test run, as seen in Figure 7. Figures 7, and 9 show also pretty better agreement with the experimental results in terms of B_{ic} fittings.

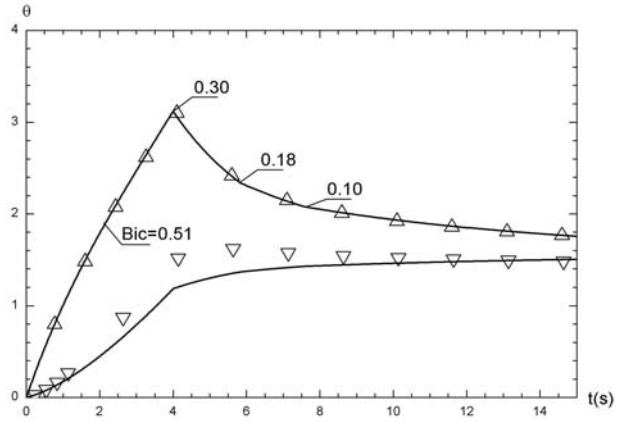

Figure 9. Predicted temperature distributions in the tube (upper) and the wire (lower) fitted piecewise with parameter B_{ic}, compared to the experimental results of the temperature in the outer surface of the tube, obtained in the second test, for $\Delta t_c = 4s$ and $I = 2{,}72kA$

5. Conclusions

The present paper reports a general solution for the heat transfer problem that describes the heating and cooling effects during the short-circuit test of on OPGW made of an aluminum tube involved by armored galvanized steel wires. It is shown that the thermal contact angle of the contact interface between the tube and the wires may play an important role in the design of this type of conductor. Temperature gradient effects in the wires may be significant in predicting the maximum temperature achieved in the tube. For the present case, gradient effects may contribute to the maximum temperature around 25°C, or 11% of the maximum temperature. Therefore, thermal capacitance based models may underestimate the maximum temperature achieved in aluminum-galvanized steel wires conductors. It is also shown that the cooling of the conductor that follows the short-circuit test cannot be satisfactorily described by a single value of the thermal contact resistance parameter. The thermal contact resistance is shown to vary while the tube cools down.

6. References

[1] S. Colle and M. de A. Andrade, “On the thermal contact resistance effects in aluminum-galvanized steel wires OPGW

submitted to a short-circuit test" *Proceeding of the 53rd IWCS / Focus Conference, Philadelphia, Pa., USA* , (2004).

[2] M. Zunec, F. Jakl and I. Ticar, "Skin effect impacto on current density distribution in OPGW cables" *Electrotechnical Review,* 70 (1-2): 17-21, (2003).

[3] I. Stakgold, "Boundary Value Problems of Mathematical Physics – Vol. II," *Macmillan*, (1968)

[4] S. Colle, "Technical Reports No. 1-5 to Pirelli Telecommunication Cables and Systems of Brazil," *Department of Mechanical Engineering, UFSC*, (2002-2003).

[5] R. S. Madge, S. Barret and H. Grad, "Performance of Optical Wires During Fault Current Tests", *IEE Transactions on Power Delivery*, 4 (3), (July, 1989).

[6] F. Jakl and A. Jakl, "Investigation of Temperature Rise of ACSR Conductors and OPGW under Short – Circuit Conditions," *CIGREE WG12*, No. 22-96.

Appendix

A.1. Solution by the Green's Function Method

The Green's function for the Neumann problem, according to the dimensionless variables taken here is the solution of the following partial differential equation

$$-\frac{1}{\eta}\frac{\partial}{\partial\eta}\left(\eta\frac{\partial g}{\partial\eta}\right)+\frac{1}{F_{oa}}\frac{\partial g}{\partial\tau}=\frac{\delta(\eta-\eta')\delta(\varphi-\varphi')}{\eta F_{oa}}-\frac{2}{\pi} \quad \text{(A1)}$$

satisfying the following boundary conditions,

$$\frac{\partial g}{\partial\varphi}=0 \text{ for } \varphi=0 \text{ and } 0\le\eta\le 1 \quad \text{(A2)}$$

$$\left.\frac{\partial g}{\partial\varphi}\right|_{\varphi=0}=\left.\frac{\partial g}{\partial\varphi}\right|_{\varphi=\pi} \quad \text{(A3)}$$

and the initial condition given by

$$g(\eta,\varphi,\tau;\eta',\varphi',\tau)=0 \quad \text{(A4)}$$

Physically, the Green´s function means a 2D temperature distribution over a semi-circle region, due to a concentrated infinite heat source located at the point given by η' and φ', for vanishing heat flux at the boundary of the region.

The solution of equation (A1) satisfying the boundary conditions (A2) and (A3) and the initial condition given by equation (A4) is the following [3,4].

$$\begin{aligned} g(\eta,\varphi,\tau;\eta',\varphi',\tau') &= \frac{2}{\pi}+\frac{2}{\pi}\sum_{m=1}^{\infty}e^{-\beta_m^{0\,2}F_{oa}(\tau-\tau')} \\ &\times\frac{J_o(\beta_m^0\eta)J_o(\beta_m^0\eta')}{{J_o}^2(\beta_m^0)}+\frac{4}{\pi}\sum_{m,n=1}^{\infty}e^{-\beta_m^{n\,2}F_{oa}(\tau-\tau')} \\ &\times\cos(n\varphi)\cos(n\varphi')\frac{J_n(\beta_m^n\eta)J_n(\beta_m^n\eta')}{(1-n^2/\beta_m^{n\,2}){J_n}^2(\beta_m^n)} \end{aligned} \quad \text{(A5)}$$

where J_n; $n=0,1,2,...$ is the Bessel function of the first kind and integer order, where the eigen-values β_m^n are the roots of $J_n'(\beta_m^n)=0$; $n=0,1,2,....$

The temperature distribution governed by equation (2) satisfying the boundary conditions given by equations (3) and (4) and the initial condition given by equation (5) of the text can be expressed by,

$$\begin{aligned} \theta_a(\eta,\varphi,\tau) &= \int_0^{\tau}p_a\left(\theta_i,\bar{\theta}_a\right)d\tau' \\ &+F_{oa}\int_0^{\tau}\int_0^{\varphi_0}[\frac{2}{\pi}+\frac{2}{\pi}\sum_{m=1}^{\infty}e^{-\beta_m^{0\,2}F_{oa}(\tau-\tau')}\frac{J_o(\beta_m^0\eta)}{J_o(\beta_m^0)} \\ &+\frac{4}{\pi}\sum_{m,n=1}^{\infty}\frac{e^{-\beta_m^{n\,2}F_{oa}(\tau-\tau')}J_n(\beta_m^n\eta)}{(1-n^2/\beta_m^{n\,2})J_n(\beta_m^n)} \\ &\times\cos n\varphi\cos n\varphi']\times\phi(\varphi',\tau')d\tau' \end{aligned} \quad \text{(A6)}$$

A.2. Time Integration Matrices

The time integration matrices of equations (18) and (19) of the text are given by the equations bellow.

$$B_{kj}^{\pm}=\sum_{m=1}^{\infty}A_{mjk}^{\pm} \quad \text{(A7)}$$

where $A_{mjk}^{\pm}$ is evaluated by the following equations for $\beta=\beta_m^{o\,2}F_{oa}$,

$$\begin{aligned} A_{kj}^{-} &= \int_{\tau_{j-1}}^{\tau_j}e^{-\beta(\tau_k-\tau')}\phi_j^{-}(\tau')d\tau' \\ &=\frac{1}{\beta}\left[e^{-\beta(k-j)\Delta\tau}-\left(\frac{e^{-\beta(k-j)\Delta\tau}-e^{-\beta(k-j+1)\Delta\tau}}{\beta\Delta\tau}\right)\right] \end{aligned} \quad \text{(A8)}$$

for $j\le k$ and

$$\begin{aligned} A_{kj}^{+} &= \int_{\tau_j}^{\tau_{j+1}}e^{-\beta(\tau_k-\tau')}\phi_j^{+}(\tau')d\tau' \\ &=-\frac{1}{\beta}\left[e^{-\beta(k-j)\Delta\tau}+\left(\frac{e^{-\beta(k-j)\Delta\tau}-e^{-\beta(k-j-1)\Delta\tau}}{\beta\Delta\tau}\right)\right] \end{aligned} \quad \text{(A9)}$$

for $j\le k-1$, where $\Delta\tau=1/M$ and $\tau_j=j\Delta\tau$; $j=1,2,....,M$, and M is the number time intervals.

$$B_{nkj}^{\pm}=\sum_{m=1}^{\infty}\frac{A_{mkj}^{n\,\pm}}{(1-n^2/\beta_m^{n\,2})} \quad \text{(A10)}$$

where $A_{mkj}^{\pm}$ is evaluated by equations (A8) and (A9), respectively, with $\beta=\beta_m^{n\,2}F_{oa}$.

Prof. Sergio Colle
LABSOLAR / NCTS – Department of Mechanical Engineering – UFSC (Federal University of Santa Catarina)
88040-900 – Florianópolis – SC – Brazil
Bibliography:
Mechanical Engineer degree in 1970 - UFSC
Master of Science in Mechanical Engineering in 1972 – COPPE / University of Rio de Janeiro
Doctor of Science in Mechanical Engineering in 1976 – COPPE / University of Rio de Janeiro
Professor of Thermodynamics, Heat Transfer and Solar Energy – Department of Mechanical Engineering – UFSC since 1974
Consulting Engineer of PIRELLI in the field of heat transfer and applied thermodynamics
Head of LABSOLAR/NCTS.

Eng. Marcelo de Araújo Andrade
Pirelli Telecomunicações Cabos e Sistemas do Brasil AS
Avenida Pirelli, 1.100 – Éden
18103-355 – Sorocaba – SP – Brazil
Bibliography:
Was born in Florianópolis – SC, Brazil in 1965
He was graduated from Federal Univeristy of Santa Catarina
He joined Pirelli in 1988 where he in charge of Telecom Engineering and Quality.